SPANDIDOS PUBLICATIONS

INTERNATIONAL JOURNAL OF ONCOLOGY 51: 445-455, 2017

Genomic profiling of long non-coding RNA and mRNA expression associated with acquired temozolomide resistance in glioblastoma cells

HUIJUN ZENG[1*], NINGBO XU[1*], YANTING LIU[2*], BOYANG LIU[1], ZHAO YANG[1], ZHAO FU[1], CHANGLIN LIAN[1] and HONGBO GUO[1]

[1]The National Key Clinical Specialty, The Engineering Technology Research Center of Education Ministry of China, Guangdong Provincial Key Laboratory on Brain Function Repair and Regeneration, Department of Neurosurgery, Zhujiang Hospital, Southern Medical University, Guangzhou, Guangdong 510282; [2]The First College of Clinical Medical Science, China Three Gorges University, Yichang, Hubei 443002, P.R. China

Received February 7, 2017; Accepted April 18, 2017

DOI: 10.3892/ijo.2017.4033

Abstract. Temozolomide (TMZ) is an alkylating chemotherapeutic agent widely used in anti-glioma treatment. However, acquired TMZ resistance represents a major clinical challenge that leads to tumor relapse or progress. This study investigated the genomic profiles including long non-coding RNA (lncRNA) and mRNA expression associated with acquired TMZ resistance in glioblastoma (GBM) cells *in vitro*. The TMZ-resistant (TR) of GBM sub-cell lines were established through repetitive exposure to increasing TMZ concentrations *in vitro*. The differentially expressed lncRNAs and mRNAs between the parental U87 and U87TR cells were detected by human lncRNA microarray method. In this study, we identified 2,692 distinct lncRNAs demonstrating >2-fold differential expression with 1,383 lncRNAs upregulated and 1,309 lncRNAs downregulated. Moreover, 4,886 differential mRNAs displayed 2,933 mRNAs upregulated and 1,953 mRNAs downregulated. Further lncRNA classification and subgroup analysis revealed the potential functions of the lncRNA-mRNA relationship associated with the acquired TMZ resistance. Gene ontology and pathway analysis on mRNAs showed significant biological regulatory genes and pathways involved in acquired TMZ resistance. Moreover, we found the ECM-receptor interaction pathway was significantly downregulated and ECM related collagen I, fibronectin, laminin and CD44 were closely associated with the TR phenotype *in vitro*. Our findings indicate that the dysregulated lncRNAs and mRNAs identified in this work may provide novel targets for overcoming acquired TMZ resistance in GBM chemotherapy.

Correspondence to: Professor Hongbo Guo, Department of Neurosurgery, Zhujiang Hospital, Southern Medical University, Gong Ye Avenue, Guangzhou, Guangdong 510282, P.R. China
E-mail: guohongbo911@126.com

*Contributed equally

Key words: long non-coding RNA, mRNA, temozolomide, resistance, glioblastoma

Introduction

Glioblastoma (GBM) is one of the most devastating malignant neoplasms in the central nervous system with increasing risk and incidence (1). Despite recent therapeutic advances, the prognosis of patients afflicted by GBM remains poor, even with multimodal therapy including maximal surgical resection followed by concurrent radiation and chemotherapy with alkylating drugs (2). Temozolomide (TMZ), an oral alkylating agent used as the first-line therapy for GBM treatment, is frequently limited in durability of treatment response because of acquired drug resistance (3). Thus, identifying novel mechanisms underlying acquired TMZ resistance may allow for a more durable benefit from the anti-glioma properties of TMZ (4).

Long non-coding RNAs (lncRNAs), longer than 200 bp in length and lacking significant protein coding open reading frames, transcribed from intergenic and intronic regions in human genome and participating in various biological or pathological processes including cancers (5,6). In the past few years, deregulated lncRNA has been widely reported to be involved in cancer occurrence, progression and metastasis (7-9). Evidence linking lncRNAs to tumor drug resistance have also emerged (10-12). For instance, lncRNA UCA1 enhanced cisplatin resistance in bladder cancer by CREB activation (13), and lncRNA GAS5 downregulation causes trastuzumab resistance in breast cancer (14). However, few studies have focused on the occurrence and development of TMZ resistance in GBM related to lncRNAs.

In this study, we profiled the expression of lncRNAs and mRNAs in U87 TMZ-resistant (U87TR) cells compared to the parental cells by microarray method. We showed various differentially expressed lncRNAs and mRNAs and found multiple dysregulated signal pathways that associated with

TMZ resistance. These findings may provide us novel insights and potential targets for overcoming acquired TMZ resistance in GBM chemotherapy.

Materials and methods

Cell culture and TR cell establishment. The human GBM cell line U87 was obtained from the American Type Culture Collection (ATCC, USA) and U251 was purchased from the CLS Cell Lines Service GmbH (Eppelheim, Germany). The TR cells were generated by repetitive pulse exposure of U87 and U251 GBM cells to TMZ (48 h every 2 weeks) and with increasing TMZ concentrations for 6 months. For TR phenotype maintenance, U87TR and U251TR cells were alternately treated with TMZ (500 μM) for 48 h. The corresponding methods were mainly based on the previous study of Monoz *et al* (15-17) and with minor adjustment in this study. The parental and TR cells were maintained in DMEM (Hyclone, USA) with 10% (v/v) FBS (Hyclone) and 1% (v/v) penicillin/streptomycin (Gibco, USA) at 37˚C in 5% CO_2 humidified air incubator (Thermo Scientific, USA).

Cell survival assay. The parental and TR cells were plated in 96-well plate and treated with TMZ in different concentrations, respectively. After 48-h incubation, cells were replaced with fresh medium with CCK-8 solution (v/v 10%; Dojindo, Japan) and incubated at 37˚C for 2 h. Then the absorbance was measured at 450 nm (reference, 620 nm) using Multiscan GO microplate reader (Thermo Fisher Scientific, Finland). Cells without TMZ treatment were set as the control and the result was shown as cell viability ratio towards the control group.

RNA extraction and qPCR analysis. Total RNA was extracted by TRIzol reagent (Invitrogen, USA) and the absorbance was measured with OD260/280 ratio higher than 1.8. For qPCR analysis, 1 μg total RNA was subjected to the synthesis of cDNA by using RevertAid First Strand cDNA Synthesis kit (Thermo Scientific, Germany). Reactions were initiated by incubation at 65˚C for 5 min, followed by 60 min at 42˚C and terminated the reaction by heating at 70˚C for 5 min. The cDNA performed to PCR by using the Maxima SYBR Green/ROX qPCR Master Mix (Thermo Scientific, Germany). Total reaction volume (25 μl) included 12.5 μl mix (2X), 1.5 μl (10 mM) primers (Table I) synthesized by Sangon Biological Engineering Technology and Services Co., Ltd. (Shanghai, China), 8.5 μl nuclease-free water and 0.8 μg/1 μl cDNA. PCR reaction was run in Step-one Plus Real-Time PCR system (Applied Biosystems, Germany) and analyzed using Step-one software. The qPCR protocol contained initial denaturation at 95˚C 10 min, then 40 cycles including 95˚C for 5-sec denaturation, 60˚C for 30 sec annealing and 72˚C for 30-sec extension. qPCR assays were carried out in triplicate, and the specificity of the PCR products was verified with melting curve analysis. The amount of each respective amplification product was determined relative to the gene β-actin. The fold change in gene expression relative to control was calculated by $2^{-\Delta\Delta CT}$ (18).

Microarray profiling and data analysis. For microarray, Arraystar Human LncRNA Microarray V3.0 covering ~30,586 lncRNAs and 26,109 coding transcripts was designed to detect the profile of human lncRNAs and protein-coding transcripts. Sample labeling and array hybridization were performed according to the Agilent One-Color Microarray-Based Gene Expression Analysis protocol (Agilent Technology). The array images were further analyzed by Agilent Feature Extraction software (version 11.0.1.1). Quantile normalization and subsequent data processing were applied with GeneSpring GX v11.5.1 software (Agilent Technologies). Distinct lncRNAs and mRNAs between U87 and U87TR were presented by hierarchical clustering and volcano plot filtering. The gene ontology (GO) analysis and pathway analysis were performed in the standard enrichment computation method according to the latest KEGG database (Kyoto Encyclopedia of Genes and Genomes, http:/www.genome.jp/kegg).

Western blot analysis. Total protein of cells was extracted by Cell Lysis and Protein Extraction kit (Keygen Biotech Co., China) and concentration was measured by a BCA Protein Detection kit (Keygen Biotech). Total protein (40 μg) was subjected to 10% SDS-polyacrylamide gel electrophoresis and transferred to PVDF membrane (Millipore Corp., USA). The blots were blocked for 1 h at RT with 5% non-fat milk (Bio-Rad, USA) in Tris-buffered saline containing 0.1% Tween-20 (TBST) and probed with following primary antibodies: MDR1/ABCB1(E1Y7B) (142 kDa), MRP1/ABCC1(D708N) (173 kDa), ABCG (66 kDa) (Cell Signaling Technology, USA), MGMT (25 kDa), collagen I (139 kDa), fibronectin (262 kDa), laminin (198 kDa) (Abcam, USA), CD44 (82 kDa) (Abnova, USA) in 5% non-fat milk in TBST overnight at 4˚C. Anti-GAPDH antibody (37 kDa) (Cell Signaling Technology) was used as a loading control. Subsequently, the blots were washed in TBST and incubated with goat anti-rabbit or mouse IgG (H+L) horseradish peroxidase-conjugated secondary antibody (Fdbio, China) for 1 h at RT. Then the blots were washed with TBST and visualized using Immobilon Western HRP Substrate (Millipore).

Enzyme-linked immunosorbent assay (ELISA). During 3-day TMZ treatment, the culture supernatants of U87 and U87TR cells were collected respectively and the level of total collagen I was measured with Collagen I ELISA kit (R&D Systems, USA). The assay was carried out as recommended by the kit protocol.

Immunofluorescence staining. For immunofluorescence analysis, GBM cells were seeded on glass coverslips (0.17 mm thickness, 14 mm diameter) in 6-well plate overnight and then treated with TMZ for 3 days, respectively. After treatments, cells were performed by PBS washing, 4% paraformaldehyde fixation (30 min), 0.1% Triton X-100 permeating (5 min) and 2% bovine serum albumin (BSA) blocking (30 min). Then the cells were incubated with anti-collagen I antibody (1:2,000) and anti-CD44 antibody (1:1,000) diluted in 2% BSA at 4˚C overnight. After 3 times PBS rinsing, appropriate fluorescent secondary antibodies were added to cell samples and incubated at 37˚C in the dark for 1 h. Coverslips were mounted on slides using mounting medium (Santa Cruz, USA) containing DAPI DNA counterstain. Images were captured by a fluorescence microscopy (IX-70, Olympus, Japan).

Table I. Primers used to perform qPCR analysis.

mRNA name	Forward primer (5'-3')	Reverse primer (5'-3')
ABCB1	CCCATCATTGCAATAGCAGG	TGTTCAAACTTCTGCTCCTGA
ABCC	ATGTCACGTGGAATACCAGC	GAAGACTGAACTCCCTTCCT
BCRP	ATGTCACGTGGAATACCAGC	GAAGACTGAACTCCCTTCCT
MGMT	ACCGTTTGCGACTTGGTACTT	GGAGCTTTATTTCGTGCAGACC
DNMT1	ACCAGGGAGAAGGACAGG	CTCACAGACGCCACATCG
TP53	GTGGTGGTGCCCTATGAG	TGTTCCGTCCCAGTAGATTA
HIF-1A	CATCTCCATCTCCTACCCACA	CTTTTCCTGCTCTGTTTGGTG
CA9	GCTGCTTCTGGTGCCTGTC	GGAGCCCTCTTCTTCTGATTTA
Bcl2L1	TGGAACTCTATGGGAACAATG	TGAGCCCAGCAGAACCAC
VEGFA	TTGCCTTGCTGCTCTACC	ATGTCCACCAGGGTCTCG
GAPDH	GACCTGACCTGCCGTCTA	AGGAGTGGGTGTCGCTGT

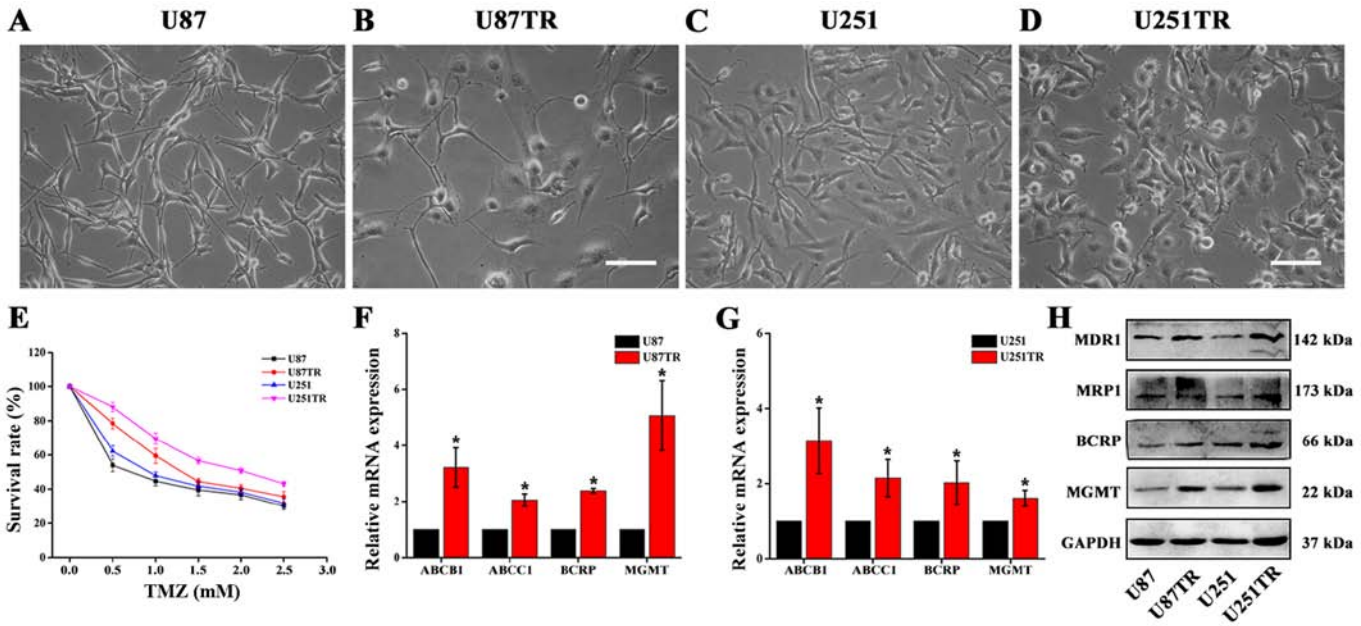

Figure 1. TMZ-resistant phenotype in U87TR and U251TR cells. The cellular morphology of U87, U87TR cells (A and B) and U251, U251TR cells (C and D), scale bar, 250 μM. The parental and TR cells were plated in 96-well plate and treated with TMZ in different concentrations. After 48-h incubation, CCK-8 assay was applied to analyze the chemosensitivity of parental and TR cells to TMZ (E). qPCR analysis of multidrug-resistant phenotype (ABCB1, ABCC1 and BCRP) and MGMT gene expression in U87TR and U251TR cells compared to the parental cells (F and G), $^{*}p<0.05$ vs. U87 or U251 parental cells. Western blot analysis of MDR phenotype and MGMT expression in GBM parental and TR cells (H).

Statistical analysis. Results are presented as mean ± standard deviation (SD) for three separate experiments and analyzed by SPSS 13.0 software with two-sample t-test assuming unequal variances. $p<0.05$ was considered as statistically significant.

Results

TMZ-resistant phenotype in U87TR and U251TR cells. U87 and U251 GBM cells were repetitively pulse-exposed to increasing TMZ concentrations for 6 months until a stable resistant phenotype was obtained. Through light microscopy, we observed that the cellular morphology of U87TR and U251TR cells differed from its parental cells with larger, irregular morphology and long protrusions (Fig. 1A-D), especially in U87TR cells. To examine the chemoresistant properties, CCK-8 assay was used to characterize chemosensitivity of these cells to TMZ. We noted that TMZ led to a concentration-dependent decrease in both TR and parental cells and the TR cells showed higer resistant level towards TMZ (U87TR 1.74±0.15 mM, U251TR 2.43±0.01 mM) when compared to its conterpart parental cells (Fig. 1E). Additionally, the expression of related multidrug-resistant (MDR) phenotypes was also analyzed by qPCR and western blot analyses. As shown in Fig. 1F and G, we found the expression of ATP-binding cassette transporters (ABCB1, ABCC and BCRP) and MGMT were significantly upregulated in TR cells and further protein analysis comfirmed these results (Fig. 1H). Together, we demonstrated that repetitive pulse-exposure of TMZ to GBM cells could establish stable TR phenotype and these sublines were suitable for further experiments.

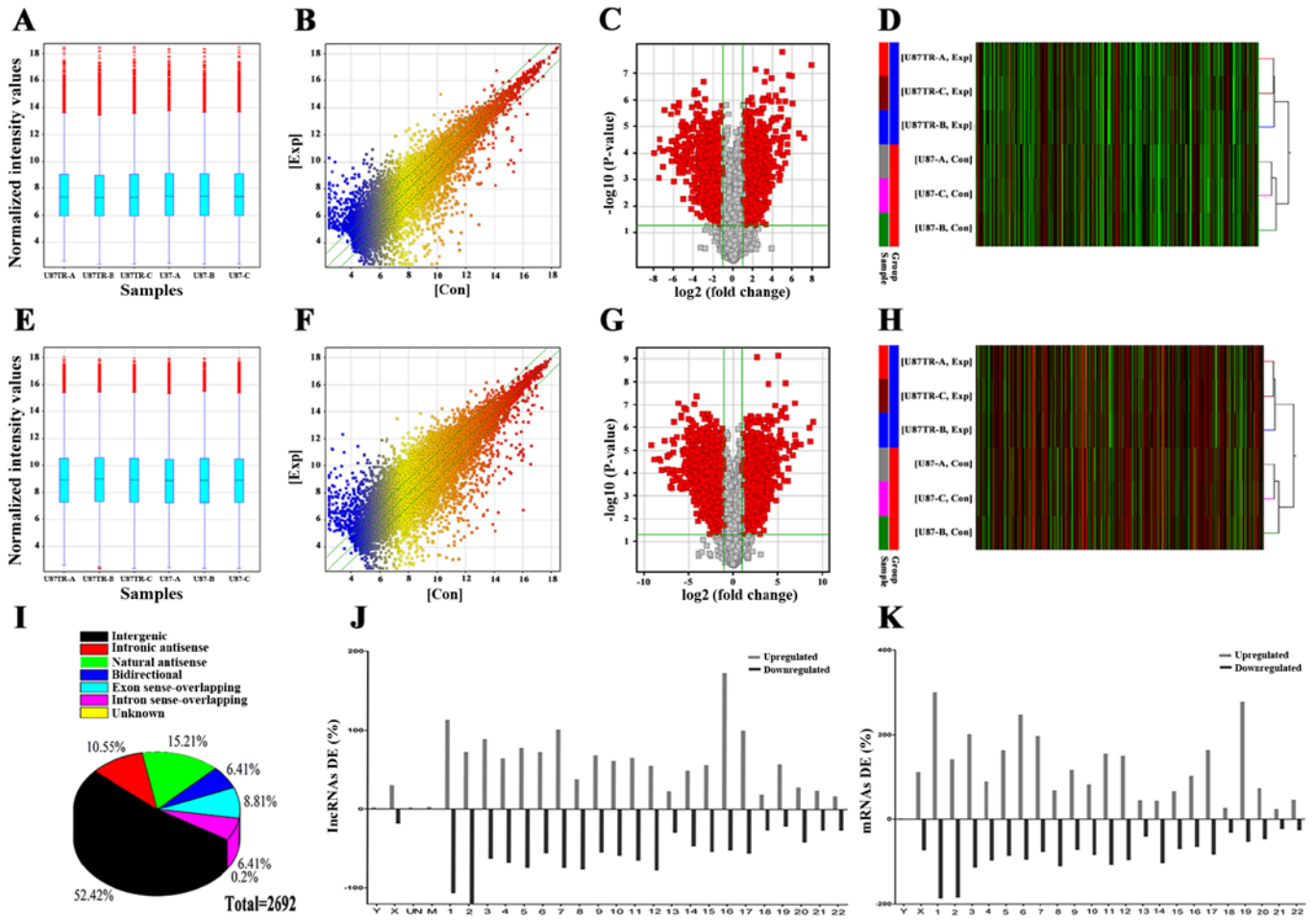

Figure 2. Differentially expressed lncRNA and mRNA profiles in U87TR cells. The box plot, scatter plot and volcano plot were used for quality assessment of lncRNA (A-C) and mRNA (E-G) data after filtering. The hierarchical clustering and heat map of lncRNA (D) and mRNAs (H) expression between U87 and U87TR. The relative higher expression levels are indicated with red and lower with green. The subgroups of distinctly expressed lncRNAs categorized by relationship (I) and distribution of aberrantly expressed lncRNA (J) and mRNA (K) profiles on human chromosomes.

Differential expression of lncRNAs and mRNAs in U87TR compared to U87 cells. Arraystar probe dataset was applied to screen differentially expressed lncRNAs and mRNAs in U87 and U87TR cells. After normalization and data filtering (Fig. 2A-C and E-G), we found that 2,692 distinct lncRNAs demonstrated >2-fold differential expression with 1,383 lncRNAs upregulated and 1,309 lncRNAs downregulated (Fig. 2D), whereas, 4,886 differential mRNAs displayed 2,933 mRNAs upregulated and 1953 mRNAs downregulated which was shown by the hierarchical clustering (fold change ≥2.0 and p-value ≤0.05) (Fig. 2H). The top 10 significantly and dominant dysregulated lncRNAs and mRNAs are listed (Tables II and III). Among the distinct lncRNAs, there were 1,410 intergenic, 284 intronic antisense, 409 natural antisense, 173 bidirectional, 238 exon sense and 173 intron sense-overlapping (Fig. 2I). Additionally, the chromosomal imbalances associated with drug resistance was analyzed and aberrantly expressed lncRNAs and mRNAs located on chromosome 1 were uneven with 8.90% in lncRNA and 10.02% in mRNA (Fig. 2J and K).

LncRNAs classification and subgroup analysis. For further investigation of potential-function of lncRNAs, lncRNAs classification and subgroup analysis were conducted. According to the Gencode annotation, lncRNAs were devided into enhancer-like lncRNAs, large intergenic non-coding RNAs (lincRNAs) and HOX lncRNAs. In enhancer lncRNA profiling, we found 108 distinct enhancer lncRNAs with 266 nearby coding genes transcription (distance <300 kb) and among these lncRNA-mRNA relationships, up-up direction (87 pairs), up-down direction (67 pairs), down-up direction (56 pairs), down-down direction (56 pairs) (Table IV). However, in lincRNA profiling, there were 809 distinct lincRNAs with 1,918 differentially expressed nearby coding genes (distance <300 kb) including up-up direction (814 pairs), up-down direction (272 pairs), down-up direction (394 pairs) and down-down direction (438 pairs) of lncRNA-mRNA relationship (Table V). The data also showed 125 HOX cluster transcribed regions in the four human HOX loci of both lncRNAs and coding transcripts including 48 coding transcripts and 77 non-coding transcripts (Table VI).

GO and pathway analysis of differentially expressed mRNAs. Previous studies have revealed that the coding and non-coding RNA can interact with each other in gene expression and dictate final protein output (19,20). To better understand the

Table II. Top 10 up- and downregulated lncRNAs in U87TR cells.

Seqname	Gene symbol	Fold change	Chromosome strand	Relationship	p-value	Up/down
ENST00000443252	AL132709.5	239.63	chr14+	Intergenic	4.79E-08	Up
uc010ahe.1	BC041856	141.54	chr14-	Intergenic	2.58E-05	Up
TCONS_00008977	XLOC_003829	99.74	chr4+	Intergenic	1.76E-05	Up
TCONS_00022632	XLOC_010933	64.73	chr14+	Intergenic	1.27E-06	Up
ENST00000556720	AL132709.5	59.33	chr14+	Intergenic	1.19E-07	Up
ENST00000513211	RP11-734I18.1	48.96	chr4+	Intergenic	1.16E-07	Up
TCONS_00027642	XLOC_013181	47.55	chr19+	Intergenic	9.62E-06	Up
ENST00000570409	RP11-461A8.4	46.57	chr16-	Intronic antisense	5.7E-06	Up
ENST00000547898	RP11-328C8.5	45.69	chr12-	Intron sense	2.39E-05	Up
ENST00000442197	AL132709.8	44.46	chr14+	Intergenic	4.36E-05	Up
NR_033869	LOC401164	264.52	chr4+	Intergenic	9.29E-05	Down
NR_038848	LOC643401	181.11	chr5+	Intergenic	0.000837	Down
ENST00000565689	RP11-941F15.1	176.55	chr15-	Intergenic	6.18E-05	Down
ENST00000444963	AC018866.1	171.92	chr2-	Intergenic	2.82E-05	Down
uc003jgv.2	LOC643401	137.76	chr5+	Intergenic	7.83E-05	Down
uc003jgx.2	LOC643401	136.05	chr5+	Intergenic	0.000304	Down
ENST00000503458	RP11-219G10.3	120.27	chr4+	Intergenic	2.19E-06	Down
ENST00000421067	RP11-83J21.3	90.59	chr9+	Intronic antisense	6.65E-05	Down
ENST00000421067	RP11-83J21.3	90.59	chr9+	Intronic antisense	6.65E-05	Down
ENST00000578278	RP11-146G7.3	77.20	chr18-	Intergenic	3.3E-06	Down

Table III. Top 10 up- and downregulated mRNAs in U87TR cells.

Gene symbol	Fold change	Up/down	p-value	Description
IL18	490.19	Up	5.32535E-07	Interleukin 18 (interferon-γ-inducing factor)
ZNF93	394.98	Up	3.9652E-06	Zinc finger protein 93
MTAP	371.14	Up	9.4726E-07	S-methyl-5'-thioadenosine phosphorylase
ZNF254	182.70	Up	5.17967E-06	Zinc finger protein 254
SOX2	129.30	Up	3.85212E-06	Transcription factor SOX-2
ZNF765	121.16	Up	2.0173E-06	Zinc finger protein 765
ZNF845	120.54	Up	6.692E-06	Zinc finger protein 845
ZNF611	118.25	Up	8.22434E-08	Zinc finger protein 611
GPR160	106.29	Up	5.8696E-06	Probable G-protein coupled receptor 160
ZNF675	99.27	Up	1.49803E-05	Zinc finger protein 675
TFPI2	607.04	Down	5.48207E-06	Tissue factor pathway inhibitor 2 precursor
BAALC	471.68	Down	2.4074E-05	Brain and acute leukemia cytoplasmic protein 2
DPP4	330.97	Down	2.21878E-05	Dipeptidyl peptidase 4
AHR	292.93	Down	2.83673E-05	Aryl hydrocarbon receptor precursor
KYNU	255.58	Down	6.99952E-05	Kynureninase isoform b
BDKRB1	206.12	Down	3.58205E-06	B1 bradykinin receptor
FOXD1	168.72	Down	6.46324E-05	Forkhead box protein D1
EREG	165.81	Down	1.73919E-05	Proepiregulin preproprotein
KYNU	161.95	Down	1.72429E-05	Kynureninase isoform a
DCN	142.10	Down	1.4439E-05	Decorin isoform b precursor

function of distinct lncRNAs, we first performed GO function analysis associating differentially expressed mRNAs with GO categories. The GO categories were generally comprised of 3 structured networks: biological processes, cellular components and molecular function (21). In our study, the differentially expressed mRNAs were mainly enriched for GO terms related to the nucleic acid metabolic process and response to chemical stimulus involved in biological processes, nucleus

Table IV. Top 10 distinct enhancer lncRNAs near the coding gene data.

Gene symbol	Fold change	Regulation - lncRNAs	Genome relationship	Nearby gene	Fold change	Regulation - mRNAs
RP11-346D6.6	39.582054	Up	Downstream	PRKG1	38.59571	Down
RP11-346D6.6	39.582054	Up	Downstream	PRKG1	10.437759	Down
RP11-346D6.6	39.582054	Up	Downstream	DKK1	2.0498126	Up
RP4-737E23.2	39.0317	Down	Downstream	NXT1	2.1266758	Up
RP4-737E23.2	39.0317	Down	Downstream	GZF1	2.2363193	Up
AX746690	28.182703	Up	Upstream	ADIG	5.036083	Down
RP13-16H11.2	27.392548	Down	Upstream	ABI1	2.0226862	Down
RP13-16H11.2	27.392548	Down	Upstream	ABI1	2.0447593	Down
RP13-16H11.2	27.392548	Down	Upstream	ABI1	2.2119737	Down
RP11-117P22.1	25.868437	Up	Upstream	AKR1C1	5.1898365	Down
RP11-445H22.4	20.70799	Down	Downstream	ADA	2.115311	Down
RP11-445H22.4	20.70799	Down	Downstream	PKIG	2.4809623	Down
RP11-445H22.4	20.70799	Down	Upstream	WISP2	2.2126765	Down
XXyac-YM21GA2.4	20.248714	Down	Upstream	CTSL1	4.7252097	Down
RP11-160A10.2	15.469184	Down	Upstream	CLVS2	8.49382	Down
LOC285758	14.293567	Up	Downstream	MARCKS	2.3576546	Up
LOC285758	14.293567	Up	Upstream	HDAC2	2.666347	Up
RP11-14N7.2	13.172412	Down	Upstream	NBPF16	2.5870576	Up

Table V. Top 10 distinct lincRNAs near the coding gene data.

Gene symbol	Fold change	Regulation lncRNAs	Genome relationship	Nearby gene	Fold change mRNAs
RP11-941F15.1	176.5588	Down	Downstream	CD276	3.1752949
RP11-146G7.3	77.20038	Down	Downstream	ARHGAP28	5.5441136
RP11-554A11.4	64.153145	Down	Downstream	CPT1A	3.7187796
RP11-554A11.4	64.153145	Down	Downstream	CPT1A	2.3309202
RP11-554A11.4	64.153145	Down	Upstream	MRGPRF	2.9983652
RP11-113C12.3	52.048756	Down	Upstream	C3AR1	4.6431336
XLOC_013181	47.557842	Up	Downstream	ZNF8	3.150816
XLOC_013181	47.557842	Up	Downstream	TRIM28	2.829188
XLOC_013181	47.557842	Up	Downstream	ZNF324	2.4305477
XLOC_013181	47.557842	Up	Upstream	ZNF544	30.045504
XLOC_013181	47.557842	Up	Upstream	ZNF274	2.003165
XLOC_013181	47.557842	Up	Upstream	ZNF274	4.3925347
PRORSD1P	46.21162	Down	Upstream	RTN4	2.7800567
PRORSD1P	46.21162	Down	Upstream	RTN4	2.2093842
PRORSD1P	46.21162	Down	Upstream	CLHC1	2.0670087
PRORSD1P	46.21162	Down	Upstream	RTN4	3.4394581
AC003092.1	43.996338	Down	Upstream	BET1	2.096403
AC003092.1	43.996338	Down	Upstream	TFPI2	607.0495
AK123141	43.92919	Up	Downstream	ZNF680	5.060253
AK123141	43.92919	Up	Downstream	ZNF680	29.15355
AK123141	43.92919	Up	Upstream	ZNF736	11.060797
AK123141	43.92919	Up	Upstream	ZNF679	3.0256562
AK123141	43.92919	Up	Upstream	ZNF727	39.63797
AK123141	43.92919	Up	Upstream	ZNF735	4.4493775
RP11-346D6.6	39.582054	Up	Downstream	PRKG1	38.59571
RP11-346D6.6	39.582054	Up	Downstream	PRKG1	10.437759
RP11-346D6.6	39.582054	Up	Downstream	DKK1	2.0498126
RP4-737E23.2	39.0317	Down	Downstream	NXT1	2.1266758
RP4-737E23.2	39.0317	Down	Downstream	GZF1	2.2363193

Table VI. HOX cluster profiling (part).

Probe name	Seqname	Gene symbol	Product
ASHGA5P021981	NM_014212	HOXC11	Homeobox protein Hox-C11
ASHGA5P053003	NM_006735	HOXA2	Homeobox protein Hox-A2
ASHGA5P005899	NM_024017	HOXB9	Homeobox protein Hox-B9
ASHGA5P032505	NM_024015	HOXB4	Homeobox protein Hox-B4
ASHGA5P036264	NM_002148	HOXD10	Homeobox protein Hox-D10
ASHGA5P053006	NM_006896	HOXA7	Homeobox protein Hox-A7
ASHGA5P036265	NM_014213	HOXD9	Homeobox protein Hox-D9
ASHGA5P032508	NM_032391	PRAC	small nuclear protein PRAC
ASHGA5P032507	NM_004502	HOXB7	Homeobox protein Hox-B7
ASHGA5P036262	NM_021192	HOXD11	Homeobox protein Hox-D11
ASHGA5P042956	NM_024014	HOXA6	Homeobox protein Hox-A6
ASHGA5P028030	NM_017410	HOXC13	Homeobox protein Hox-C13
ASHGA5P001267	NM_018952	HOXB6	Homeobox protein Hox-B6
ASHGA5P055442	NM_153693	HOXC6	Homeobox protein Hox-C6 isoform 2
ASHGA5P042958	NM_005523	HOXA11	Homeobox protein Hox-A11
ASHGA5P006323	NM_030661	HOXA3	Homeobox protein Hox-A3 isoform a

Table VII. Significant pathways associated with TMZ resistance.

Pathway ID	Definition	Fisher p-value	FDR	Enrichment score	Genes
hsa03430	Mismatch repair (MMR)	7E-07	2E-05	6.16	EXO1/LIG1/MLH1/MSH3/PCNA/ POLD2/POLD3/RFC2/RFC3/ RFC4/RFC5/RPA1/RPA2
hsa03420	Nucleotide excision repair (NER)	3E-05	0.001	4.48	ERCC1/ERCC2/ERCC3/ERCC8/ POLD3/POLE/POLE2/RFC2/ RFC3/RFC4/RFC5/RPA1/RPA2
hsa04512	ECM-receptor interaction	2E-07	3E-05	6.60	CD44/CD47/COL1A1/COL1A2/ COL3A1/COL4A5/COL5A1/ COL5A2/COL6A1/COL6A2/COL6A3/ FN1/HSPG2/ITGA1/ITGA11/ ITGA5/ITGAV/ITGB1/LAMA2/ LAMA4/LAMC1/LAMC2/SPP1

and extracellular region part involved in cellular components as well as nucleic acid binding and protein binding involved in molecular function (Figs. 3A-C and 4A-C).

To identify significant pathways associated with TMZ resistance, pathway analysis was applied for the differentially expressed mRNAs. We found a total of 97 pathways that showed significant differences with 28 upregulated and 69 downregulated pathways. The top 3 upregulated pathways were pyrimidine metabolism, RNA transport and DNA replication signaling while the top 3 downregulated pathways were rheumatoid arthritis, ECM-receptor interaction and leishmaniasis signaling. The predominant pathways are shown in (Figs. 3D and 4D) and it is noteworthy that the validated MMR and NER pathways, which associated with TMZ resistance, were upregulated with the false discovery rate of Pathway ID at $2.298x10^{-5}$ and $9.769x10^{-4}$, respectively (Table VII).

Downregulation of ECM-receptor interaction pathway associated with TR phenotype. For microarray profile validation, six mRNAs (DNMT1, TP53, HIF-1A, CA9, Bcl2L1 and VEGFA) were randomly selected and performed for qPCR analysis in U87 and U87TR cells. Results showed that the DNMT1, TP53 and Bcl2L1 were significantly upregulated while the HIF-1A, CA9 and VEGFA were downregulated compared to the parental U87 cells (Fig. 5A). With the distinct cellular morphology (Fig. 1) and downregulation of ECM-related pathway (Fig. 4D) in TR cells, we speculated that the ECM-related cellular morphology alterations may associate with the TR properties. In the downregulated ECM-receptor interaction pathway,

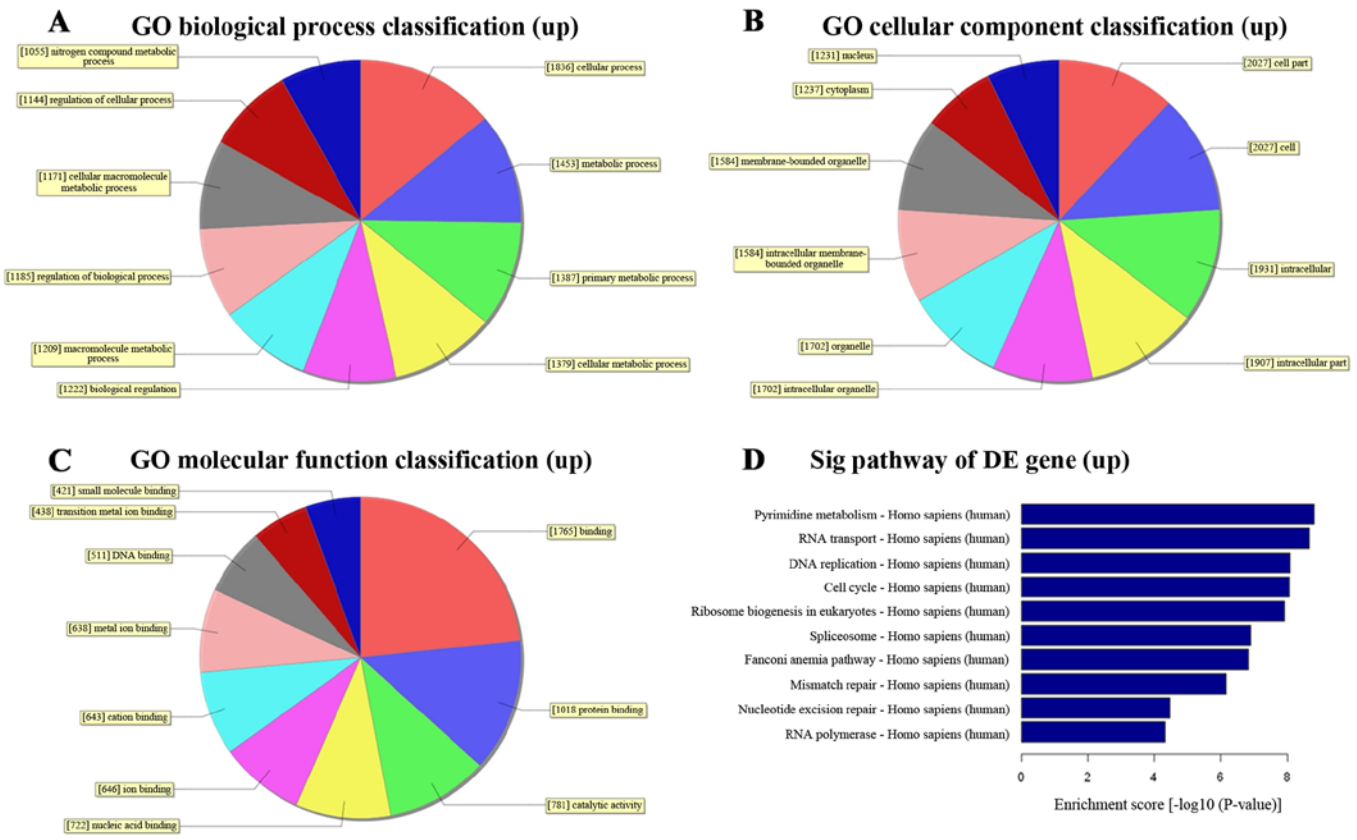

Figure 3. GO and pathway analysis on functional classification of upregulated genes. GO categories cover three domains: biological process (A), cellular component (B) and molecular function (C). Analysis of significantly upregulated pathways (D). The (-log10) p-value indicates the significance of pathway correlated enrichment in the differentially expressed mRNAs.

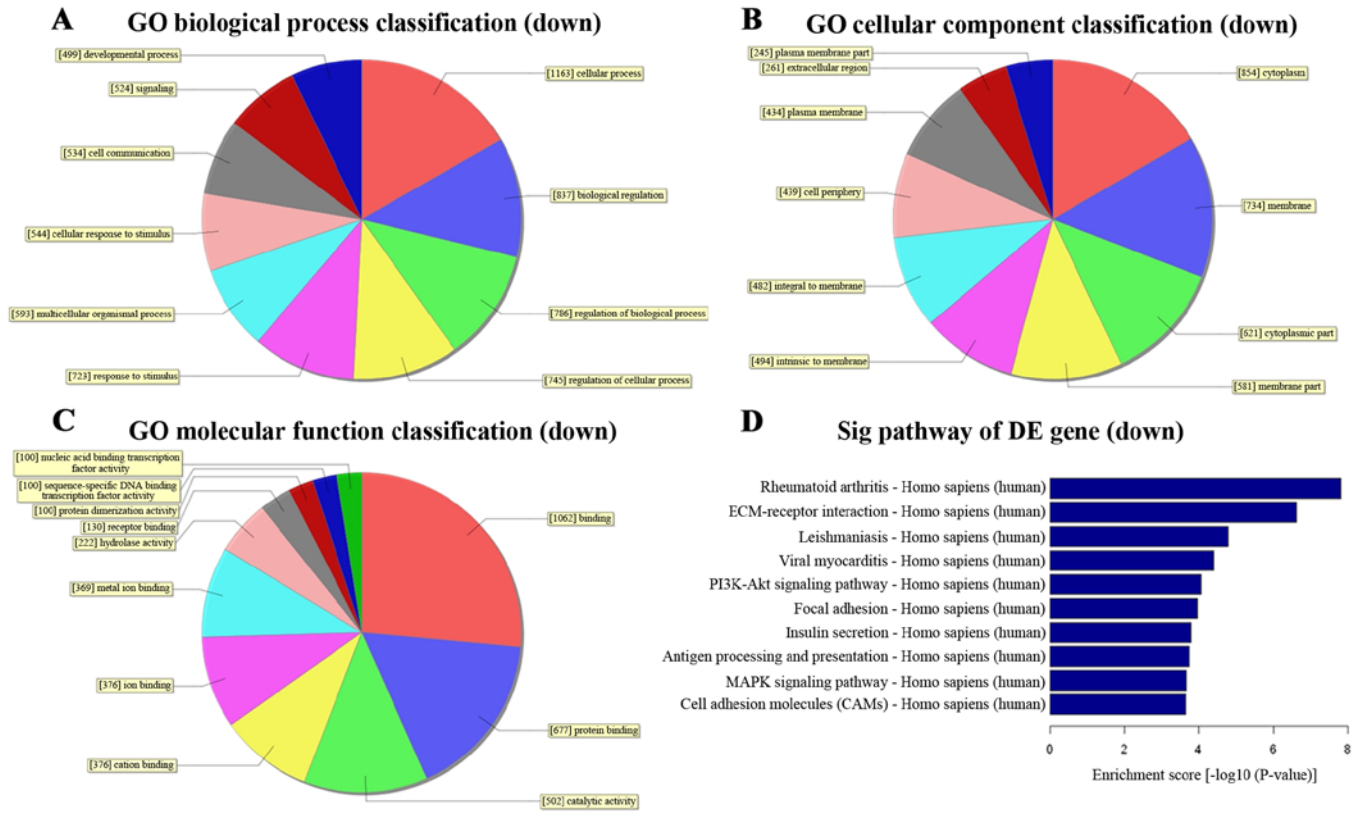

Figure 4. GO and pathway analysis on functional classification of downregulated genes. GO categories cover three domains: biological process (A), cellular component (B) and molecular function (C). Analysis of significant downregulated pathways (D). The (-log10) p-value indicates the significance of pathway correlated enrichment in the differentially expressed mRNAs.

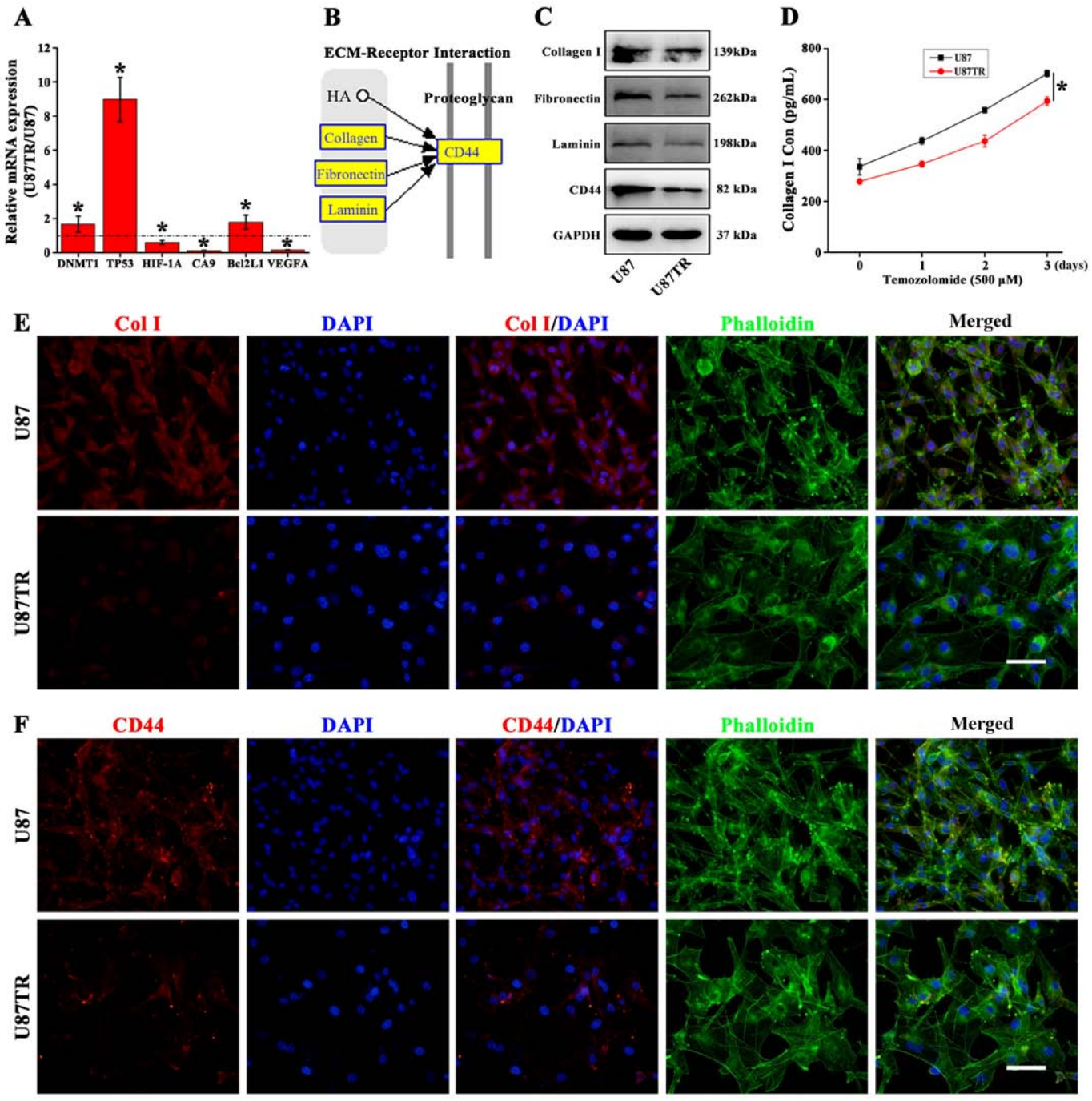

Figure 5. ECM-receptor interaction pathway downregulation in GBM TR cells. Microarray profile validation on mRNA expression by qPCR analysis (A), *p<0.05 vs. U87 parental cells. The ECM-receptor interaction pathway from the KEGG database (B). Western blot analysis on ECM-related proteins in U87 and U87TR cells (C). ELISA analysis of collagen I protein expression in TMZ (500 μM) treated U87 and U87TR cell culture supernatants during 3 days, *p<0.05 vs. U87 parental cells (D). The U87 and U87TR cells were plated in 6-well plate overnight and then treated with 500 μM TMZ. After 3-day incubation, immunofluorescence staining was used to analysis collagen I (E) and CD44 (F) expression in U87 and U87TR cells, scale bar, 50 μM..

we found collagen, integrin and laminin expression down-regulated with cell-surface glycoprotein CD44 and CD47 (Table VII). Moreover, the ECM related receptor interaction from the KEGG Pathway Database revealed that collagen, fibronectin and laminin could enhance its downstream CD44 expression (Fig. 5B). To verify this, western blot analysis was applied and the results showed the protein expression of collagen I, fibronectin, laminin and CD44 were significantly decreased in U87TR cells as compared to parental U87 cells (Fig. 5C). To comfirm this, ELISA assay was used to analyze the collagen I expression in TMZ treated U87 and U87TR cell supernatants during 3 days. The results showed U87TR cells with significant downregulated collagen I expression when compared to the parental U87 cells during TMZ treatment (Fig. 5D). In addition, the expression of collagen I and CD44 were further confirmed by immunofluorescence staining. Data showed that the U87TR cells presented with relative larger and irregular cytoskeleton (phalloidin in green), decreased secretion of collagen I (Fig. 5E) and weaker CD44 expression (Fig. 5F). Together, these results indicated that the TR

phenotype was associated with the downregulation of ECM signaling and ECM-related collagen or CD44 may act as TR phenotype molecular markers.

Discussion

The emergence of acquired drug resistance in tumor constantly leads to chemotherapy faliure or even tumor relapse. Thus, fully understanding its mechanisms is urgent for improving effective chemotherapy and overcoming tumor drug resistance. Here, we sought to explore the mechanisms of acquired resistance to TMZ in GBM through *in vitro* TMZ-resistant GBM cell lines generated by repetitive exposure to increasing TMZ concentrations. Although this approach may not closely reflect the situation *in vivo*, it allows us for an assessment of mechanisms triggered by repeated pulse-exposure to TMZ chemotherapy *in vitro*.

Previous studies have indicated a growing number of molecular mechanisms contributing to TMZ resistance in GBM including genetic and epigenetic, such as MGMT methylation (22), IDH mutations (23), aberrant ABC transporter expression (24,25), p53 mutations and deletions (26), DNA repair deregulation (27,28) and miRNAs (29,30). Furthermore, evidence is now beginning to demonstrate lncRNAs as having important roles in cancer therapy (31,32). However, the relationships between lncRNAs and GBM acquired TMZ resistance are rarely reported. In our study, the TMZ-resistant GBM cell lines were first generated using stepwise selection and then subjected to the Human lncRNA microarray. We found numerous distinctly expressed lncRNAs and mRNAs with up- or downregulation (Tables II and III). To our best knowledge, these results may be the first reporting on expression profile of lncRNAs and mRNAs associated with TMZ resistance in GBM cells *in vitro*.

For preliminary understanding upon these differential expressed lncRNAs and mRNAs towards TMZ resistance, further functional analysis was processed. In lncRNA classification and subgroup analysis, the lncRNAs were devided into three types, the enhancer-like lncRNAs, lincRNAs and HOX lncRNAs, and each of the function pattern was distinct. For example, lincRNAs regulate the neighboring HOX gene expression via impacting chromatin signature (33) while enhancer-like lncRNAs function by interacting with their nearby coding genes (34). Thus the exact function of lncRNA clusters is not yet clear before every single lncRNA is identified and still need further studies. According to previous studies, we also found some distinct lncRNAs in our study, which are consistent with other researchers, for example, the lncRNA CRNDE (7), UCA-1 (6,35), MEG3 (31,36) and HOTAIR (37). These suggest that the data obtained in this study are reliable. Additionally, lncRNAs were also reported to function in tumor drug resistance through coding transcription modulation (38). In our study, some function of molecules in the drug resistance related MMR and NER signaling pathway were upregulated in U87TR cells, e.g., MSH3 in MMR and ERCC1/2 in NER signaling, which were revealed by the pathway analysis on mRNAs and were consistent with previous reports (39,40).

With the great morphologic changes and downregulation of ECM-receptor interaction pathway in TR cells as compared with their parental cells, we speculate that the cell morphology change may associate with drug resistance phenotype. Previous reports demonstrated that drug resistance acquisition showed statistically significant morphological changes in cell membrane as well as biological parameters (41). Chemotherapy-induced phenotypic reversion of cancer cells is accompanied by regression of several morphological malignant features (42). Here, we have confirmed some important molecules in ECM-receptor interaction pathway, e.g., the collagen, fibronectin, laminin and CD44 were associated with TMZ resistance phenotype. In this study, we showed that the collagen, fibronectin and laminin could enhance its downstream CD44 expression in U87TR cells according to the KEGG pathway database. Chetty *et al* reported that the CD44-mediated cell matrix interaction in glioma perivascular niches enhances cancer stem cell phenotype and promote tumor aggressiveness (43). Moreover, recent studies have shown that the high level of CD44 was associated with a better survial and better response to radiotherapy and TMZ and the CD44 could establish a prognosis marker by predicting survival and response to therapy for GBM patients (44,45). In our study, the CD44 expression was downregulated in U87TR cells and targeting CD44 expression might enhance the TMZ chemosensitivity to TR cells. However, its role and underlying mechanisms are not fully understood and more effort is still needed for further studies. Therefore, these data suggest that acquired TMZ resistance might be mirrored by the parallel changes in cellular morphology associated with CD44 expression.

In conclusion, we showed differential lncRNAs and mRNAs expression profiles associated with TMZ resistance in GBM cells *in vitro*, and these dysregulated lncRNAs and mRNAs identified in this work may represent good candidates for future diagnostic or prognostic biomarkers and provide novel targets for overcoming acquired TMZ resistance in GBM chemotherapy.

Acknowledgements

This study was supported by grants from the National Natural Science Foundation of China (81672477, 81372691, 81041068 and 30971183) and Guangdong Provincial Clinical Medical Centre for Neurosurgery (no. 2013B020400005). We thank the Department of Anatomy, Key Laboratory of Construction and Detection of Guangdong Province, Southern Medical University, Guangzhou, for generous help.

References

1. Thomas AA, Brennan CW, DeAngelis LM and Omuro AM: Emerging therapies for glioblastoma. JAMA Neurol 71: 1437-1444, 2014.
2. Preusser M, de Ribaupierre S, Wöhrer A, Erridge SC, Hegi M, Weller M and Stupp R: Current concepts and management of glioblastoma. Ann Neurol 70: 9-21, 2011.
3. Stavrovskaya AA, Shushanov SS and Rybalkina EY: Problems of glioblastoma multiforme drug resistance. Biochemistry (Mosc) 81: 91-100, 2016.
4. Sarkaria JN, Kitange GJ, James CD, Plummer R, Calvert H, Weller M and Wick W: Mechanisms of chemoresistance to alkylating agents in malignant glioma. Clin Cancer Res 14: 2900-2908, 2008.
5. Gibb EA, Brown CJ and Lam WL: The functional role of long non-coding RNA in human carcinomas. Mol Cancer 10: 38, 2011.

6. Xue M, Chen W and Li X: Urothelial cancer associated 1: A long noncoding RNA with a crucial role in cancer. J Cancer Res Clin Oncol 142: 1407-1419, 2016.
7. Wang Y, Wang Y, Li J, Zhang Y, Yin H and Han B: CRNDE, a long-noncoding RNA, promotes glioma cell growth and invasion through mTOR signaling. Cancer Lett 367: 122-128, 2015.
8. Ni B, Yu X, Guo X, Fan X, Yang Z, Wu P, Yuan Z, Deng Y, Wang J, Chen D, *et al*: Increased urothelial cancer associated 1 is associated with tumor proliferation and metastasis and predicts poor prognosis in colorectal cancer. Int J Oncol 47: 1329-1338, 2015.
9. Zhang JY, Weng MZ, Song FB, Xu YG, Liu Q, Wu JY, Qin J, Jin T and Xu JM: Long noncoding RNA AFAP1-AS1 indicates a poor prognosis of hepatocellular carcinoma and promotes cell proliferation and invasion via upregulation of the RhoA/Rac2 signaling. Int J Oncol 48: 1590-1598, 2016.
10. Sun QL, Zhao CP, Wang TY, Hao XB, Wang XY, Zhang X and Li YC: Expression profile analysis of long non-coding RNA associated with vincristine resistance in colon cancer cells by next-generation sequencing. Gene 572: 79-86, 2015.
11. Parasramka MA, Maji S, Matsuda A, Yan IK and Patel T: Long non-coding RNAs as novel targets for therapy in hepatocellular carcinoma. Pharmacol Ther 161: 67-78, 2016.
12. He DX, Zhang GY, Gu XT, Mao AQ, Lu CX, Jin J, Liu DQ and Ma X: Genome-wide profiling of long non-coding RNA expression patterns in anthracycline-resistant breast cancer cells. Int J Oncol 49: 1695-1703, 2016.
13. Pan J, Li X, Wu W, Xue M, Hou H, Zhai W and Chen W: Long non-coding RNA UCA1 promotes cisplatin/gemcitabine resistance through CREB modulating miR-196a-5p in bladder cancer cells. Cancer Lett 382: 64-76, 2016.
14. Li W, Zhai L, Wang H, Liu C, Zhang J, Chen W and Wei Q: Downregulation of LncRNA GAS5 causes trastuzumab resistance in breast cancer. Oncotarget 7: 27778-27786, 2016.
15. Munoz JL, Rodriguez-Cruz V, Greco SJ, Ramkissoon SH, Ligon KL and Rameshwar P: Temozolomide resistance in glioblastoma cells occurs partly through epidermal growth factor receptor-mediated induction of connexin 43. Cell Death Dis 5: e1145, 2014.
16. Munoz JL, Rodriguez-Cruz V, Greco SJ, Nagula V, Scotto KW and Rameshwar P: Temozolomide induces the production of epidermal growth factor to regulate MDR1 expression in glioblastoma cells. Mol Cancer Ther 13: 2399-2411, 2014.
17. Munoz JL, Walker ND, Scotto KW and Rameshwar P: Temozolomide competes for P-glycoprotein and contributes to chemoresistance in glioblastoma cells. Cancer Lett 367: 69-75, 2015.
18. Livak KJ and Schmittgen TD: Analysis of relative gene expression data using real-time quantitative PCR and the 2(-Delta Delta C(T)) method. Methods 25: 402-408, 2001.
19. Guil S and Esteller M: RNA-RNA interactions in gene regulation: The coding and noncoding players. Trends Biochem Sci 40: 248-256, 2015.
20. Yan Y, Zhang L, Jiang Y, Xu T, Mei Q, Wang H, Qin R, Zou Y, Hu G, Chen J, *et al*: LncRNA and mRNA interaction study based on transcriptome profiles reveals potential core genes in the pathogenesis of human glioblastoma multiforme. J Cancer Res Clin Oncol 141: 827-838, 2015.
21. Cao G, Zhang J, Wang M, Song X, Liu W, Mao C and Lv C: Differential expression of long non-coding RNAs in bleomycin-induced lung fibrosis. Int J Mol Med 32: 355-364, 2013.
22. Fan CH, Liu WL, Cao H, Wen C, Chen L and Jiang G: O^6-methylguanine DNA methyltransferase as a promising target for the treatment of temozolomide-resistant gliomas. Cell Death Dis 4: e876, 2013.
23. Hartmann C, Hentschel B, Simon M, Westphal M, Schackert G, Tonn JC, Loeffler M, Reifenberger G, Pietsch T, von Deimling A, *et al*; German Glioma Network: Long-term survival in primary glioblastoma with versus without isocitrate dehydrogenase mutations. Clin Cancer Res 19: 5146-5157, 2013.
24. Schaich M, Kestel L, Pfirrmann M, Robel K, Illmer T, Kramer M, Dill C, Ehninger G, Schackert G and Krex D: A MDR1 (ABCB1) gene single nucleotide polymorphism predicts outcome of temozolomide treatment in glioblastoma patients. Ann Oncol 20: 175-181, 2009.
25. Lin F, de Gooijer MC, Roig EM, Buil LC, Christner SM, Beumer JH, Würdinger T, Beijnen JH and van Tellingen O: ABCB1, ABCG2, and PTEN determine the response of glioblastoma to temozolomide and ABT-888 therapy. Clin Cancer Res 20: 2703-2713, 2014.
26. Wang YY, Zhang T, Li SW, Qian TY, Fan X, Peng XX, Ma J, Wang L and Jiang T: Mapping p53 mutations in low-grade glioma: A voxel-based neuroimaging analysis. AJNR Am J Neuroradiol 36: 70-76, 2015.
27. Turner KM, Sun Y, Ji P, Granberg KJ, Bernard B, Hu L, Cogdell DE, Zhou X, Yli-Harja O, Nykter M, *et al*: Genomically amplified Akt3 activates DNA repair pathway and promotes glioma progression. Proc Natl Acad Sci USA 112: 3421-3426, 2015.
28. Trivedi RN, Almeida KH, Fornsaglio JL, Schamus S and Sobol RW: The role of base excision repair in the sensitivity and resistance to temozolomide-mediated cell death. Cancer Res 65: 6394-6400, 2005.
29. Wong ST, Zhang XQ, Zhuang JT, Chan HL, Li CH and Leung GK: MicroRNA-21 inhibition enhances in vitro chemosensitivity of temozolomide-resistant glioblastoma cells. Anticancer Res 32: 2835-2841, 2012.
30. Ujifuku K, Mitsutake N, Takakura S, Matsuse M, Saenko V, Suzuki K, Hayashi K, Matsuo T, Kamada K, Nagata I, *et al*: miR-195, miR-455-3p and miR-10a(*) are implicated in acquired temozolomide resistance in glioblastoma multiforme cells. Cancer Lett 296: 241-248, 2010.
31. Liu J, Wan L, Lu K, Sun M, Pan X, Zhang P, Lu B, Liu G and Wang Z: The long noncoding RNA MEG3 contributes to cisplatin resistance of human lung adenocarcinoma. PLoS One 10: e0114586, 2015.
32. Tsang WP, Wong TW, Cheung AH, Co CN and Kwok TT: Induction of drug resistance and transformation in human cancer cells by the noncoding RNA CUDR. RNA 13: 890-898, 2007.
33. Ulitsky I and Bartel DP: lincRNAs: Genomics, evolution, and mechanisms. Cell 154: 26-46, 2013.
34. Cheng N, Li X, Zhao C, Ren S, Chen X, Cai W, Zhao M, Zhang Y, Li J, Wang Q, *et al*: Microarray expression profile of long non-coding RNAs in EGFR-TKIs resistance of human non-small cell lung cancer. Oncol Rep 33: 833-839, 2015.
35. Fan Y, Shen B, Tan M, Mu X, Qin Y, Zhang F and Liu Y: Long non-coding RNA UCA1 increases chemoresistance of bladder cancer cells by regulating Wnt signaling. FEBS J 281: 1750-1758, 2014.
36. Li J, Bian EB, He XJ, Ma CC, Zong G, Wang HL and Zhao B: Epigenetic repression of long non-coding RNA MEG3 mediated by DNMT1 represses the p53 pathway in gliomas. Int J Oncol 48: 723-733, 2016.
37. Zhang J, Zhang P, Wang L, Piao HL and Ma L: Long non-coding RNA HOTAIR in carcinogenesis and metastasis. Acta Biochim Biophys Sin (Shanghai) 46: 1-5, 2014.
38. Xia H and Hui KM: Mechanism of cancer drug resistance and the involvement of noncoding RNAs. Curr Med Chem 21: 3029-3041, 2014.
39. Idbaih A, Carvalho Silva R, Crinière E, Marie Y, Carpentier C, Boisselier B, Taillibert S, Rousseau A, Mokhtari K, Ducray F, *et al*: Genomic changes in progression of low-grade gliomas. J Neurooncol 90: 133-140, 2008.
40. Geng P, Ou J, Li J, Liao Y, Wang N, Xie G, Sa R, Liu C, Xiang L and Liang H: A comprehensive analysis of influence ERCC polymorphisms confer on the development of brain tumors. Mol Neurobiol 53: 2705-2714, 2016.
41. Pasqualato A, Palombo A, Cucina A, Mariggiò MA, Galli L, Passaro D, Dinicola S, Proietti S, D'Anselmi F, Coluccia P, *et al*: Quantitative shape analysis of chemoresistant colon cancer cells: Correlation between morphotype and phenotype. Exp Cell Res 318: 835-846, 2012.
42. Uppal SO, Li Y, Wendt E, Cayer ML, Barnes J, Conway D, Boudreau N and Heckman CA: Pattern analysis of microtubule-polymerizing and -depolymerizing agent combinations as cancer chemotherapies. Int J Oncol 31: 1281-1291, 2007.
43. Chetty C, Vanamala SK, Gondi CS, Dinh DH, Gujrati M and Rao JS: MMP-9 induces CD44 cleavage and CD44 mediated cell migration in glioblastoma xenograft cells. Cell Signal 24: 549-559, 2012.
44. Guadagno E, Borrelli G, Califano M, Calì G, Solari D and Del Basso De Caro M: Immunohistochemical expression of stem cell markers CD44 and nestin in glioblastomas: Evaluation of their prognostic significance. Pathol Res Pract 212: 825-832, 2016.
45. Pinel B, Duchesne M, Godet J, Milin S, Berger A, Wager M and Karayan-Tapon L: Mesenchymal subtype of glioblastomas with high DNA-PKcs expression is associated with better response to radiotherapy and temozolomide. J Neurooncol 132: 287-294, 2017.